

Metal-Organic-Frameworks: Low Temperature Gas Sensing

Subjects: Nanoscience & Nanotechnology

Contributor: Noushin Nasiri

Metal-organic frameworks (MOFs), a class of porous coordination polymers (PCPs), are crystalline frameworks with open porosity and are composed of metal nodes and organic linkers. Over the last two decades, numerous compounds have been synthesised by changing the metal ions and organic ligands to produce materials with exceptional properties, including large surface area (surface areas more than 1,000 m²g⁻¹), adjustable pore size, and tunable functional groups. The manifold approaches for MOF synthesis, including the most versatile and widely used solvothermal methods, and recently realised green approaches, such as solvent-free mechanochemical routes, are making the process of preparing high-quality MOF-based materials easier and more environmentally friendly.

Keywords: metal-organic frameworks ; hybrid nanomaterials ; gas sensing

1. Introduction

In recent decades, the rapid growth of urban populations has resulted in new public health concerns and environmental pollution [1][2], and the fast monitoring of air- and water-borne contaminants using effective sensors has grown considerably in importance [1][3]. An effective sensor should interact with the target analyte selectively with high sensitivity and short response time [2][4][5][6]. In addition, the sensor should be cost-effective and demonstrate high reusability and reproducibility [2][7]. Sensors can be utilized to detect pollutants/analytes in aqueous (such as heavy metals, toxic organic compounds, and antibiotics) and gaseous form (such as volatile organic compounds, toxic gases, and greenhouse gases) [2][6][8][9]. The latter has a wide range of applications in food quality processes, industrial gases detection, and disease diagnosis, as well as indoor air-quality monitoring [8][10][11][12].

Several gas-sensing techniques have been developed including optical, capacitive, chemoresistive, and magnetic sensors [8][13][14][15][16][17][18][19][20][21][22][23][24][25][26][27][28][29][30][31][32][33]. In optical sensing, material optical properties change upon adsorption of the target analyte onto the surface producing an optical signal such as a change in visible colour, refractive index, luminescence intensity, etc. [27][32]. Capacitive-based sensors are an attractive class of sensors, in which capacitance changes due to the change in the dielectric permittivity upon adsorbing the gas/vapour molecules are detected [28][29][30]. In chemoresistive detectors, electrical conductivity changes as a result of a reaction between the target gas and oxygen molecules adsorbed on the surface of the sensing material [4][21][33]. Generally, chemoresistive-based gas sensors provide a superior sensing response at room temperature compared to optical-based gas sensors. However, their slow response dynamic at low/room operating temperature and their lack of selectivity towards target gases hinder their real-world application [4][5][6].

In magnetic gas sensors, the magnetic properties of the sensing material are changed upon exposure to the target gas molecules; the change can be measured by, for example, application of the Hall effect, magnetization, spin orientation, ferromagnetic resonance, the magneto-optical Kerr effect, or the magnetostatic wave oscillation effect [8][13][14][15][17][18][19][20][21][22][23][24][25][26][31][34][35]. Sensing materials for gas detection can be classified into metal oxides [16][36][37], conductive and non-conductive polymers [38][39][40][41], carbon-based materials (e.g., graphene, carbon nanotubes, etc.) [42][43][44][45][46], noble metal-based structures [47][48][49][50], ionic liquids [51][52][53], metal-organic frameworks [8][54][55][56], and their composites [57][58][59]. Among these material groups, metal oxide-based sensors have been investigated extensively due to their strong and rapid response, low limit of detection (LOD), high reproducibility, simple and portable design, and low fabrication cost [60][61][62]. In recent years, the development of nanostructures and nanocomposites of metal oxide sensors has further improved device sensing characteristics. Despite these advantages and improvements, high operating temperature and inadequate gas selectivity have hindered substantial growth into new markets [61][63][64]. Polymers have been utilized in gas sensors as a sensing agent (mainly in a functionalized state) or immobilizing component to overcome

some of these challenges [39][65]. Although significant progress in polymer sensors has been achieved over the last 20 years, these sensors encounter difficulties, including complex sensing mechanisms, poor selectivity towards target gases, a slow response dynamic, and significant matrix aging [22][38].

Among the unique properties of MOFs, the reversible and selective adsorption of guest molecules onto their large surface areas is of great importance for sensing applications [2][54]. In fact, a high concentration of target gases inside a highly porous structure boosts the sensitivity of the sensor and the control over functional groups and pore sizes of the framework enhances the selectivity of the detection process [54]. Furthermore, in contrast to carbon-based and metal oxide-based sensors, which require high working temperature, MOF-based sensors have shown promising performances at low/room temperatures, resulting in significant reductions in power consumption, ease of manufacture and broadened application areas [66][67][68][69]. The variation in MOFs' physical and chemical properties following the adsorption of intended gas molecules has been exploited for the effective monitoring of environmental pollutants, indoor air quality, medical diagnosis and other areas of application [8][11][29][70][71].

2. Nitrogen Dioxide (NO₂)

Among the most common pollutants, NO₂ is a harmful gas that is generated by combustion processes at high temperatures and requires to be monitored in order to control its release [72]. NO₂ is the main source of nitric acid aerosol leading to smog and acid rain; in humans, it can cause inflammation of the airways and can even cause death at high concentrations [73][74]. Therefore, there is great demand for highly sensitive, selective, cost-effective, rapid and reliable, non-invasive techniques for monitoring NO₂.

Monitoring the optical emission changes of the MOF pre- and post-NO₂ exposure provides an interesting route for the utilization of MOF-based materials in gas-sensing applications. Luminescent MOFs (LMOFs) are widely used in gas sensing because of their excellent optical response towards guest molecules inside their cavities. Gas sensors, fabricated using two lanthanide-based MOFs (Tb-MOF and Eu-MOF, formed by 2-amino-1,4-benzene dicarboxylic acid with europium and terbium salts, respectively), were reported by Gamonal et al. [75] for NO₂ gas detection with an LOD of 2.2 ppm at room temperature. The sensing mechanism was based on the rise in Eu³⁺ luminosity and the reduction in Tb³⁺ luminescence upon exposure to NO₂ gas. Zhang et al. [76] demonstrated a direct correlation between the fluorescence intensity of the ZJU-66-based sensor and NO₂ concentrations. Similarly, Moscoso et al. [77] developed Tb-based MOF films, so-called Tb(BTC)@PDMS (BTC: benzene-1,3,5-tricarboxylate, PDMS: polydimethylsiloxane), where the photoluminescent frequency of the film was gradually decreased as the NO₂ concentration was increased from 0 to 500 ppm.

A combination of colorimetric and chemoresistive MOF detectors (MOF A, with Co and octadentate calix[4]-resorcinarene as the metallic centre and ligand, respectively) was synthesised by Ma et al. [78] using a solvothermal approach. The sensing mechanism was based on the absorption of NO₂ gas molecules onto the surface of MOF A. The O atoms of the absorbed NO₂ interacted primarily with the adjacent carboxylic groups and coordinating water through hydrogen-bonding interactions, leading to the formation of a conductive pathway. Another conductive pathway may be formed by the NO₂ molecule and H₃O⁺ through hydrogen-bonding interactions (**Figure 1b**, inset), resulting in an eight orders of magnitude enhancement for conductivity where the resistance of MOF A decreased from $5.7 \times 10^{11} \Omega$ to $9.1 \times 10^3 \Omega$ upon exposure to NO₂ gas molecules (**Figure 1b**). In addition to the electrical sensing response, a visible change in the colour was observed in MOF A where the crystal colour changed from red to yellow after NO₂ exposure (**Figure 1a**).

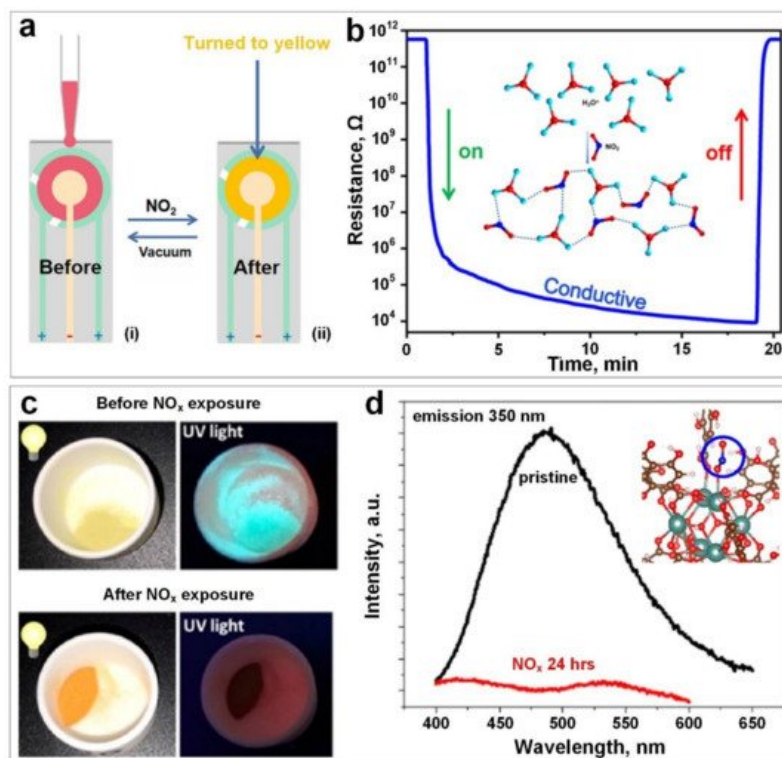


Figure 1. (a) The colour change in a gold electrode sheet covered by MOF A before and after NO_2 exposure. (b) The resistance variation versus time upon NO_2 exposure. Reproduced with permission from [79] American Chemical Society, 2021. (c) The colour change of Y-DOBDC before and after exposure to NO_x under visible and UV light. (d) Photoluminescent intensity of Y-DOBDC before and after 24 h exposure to NO_x , and the guest-framework interactions (Inset). Reproduced with permission from [32] American Chemical Society, 2019.

In a similar gas molecule absorption approach, Gallis et al. [32] reported the NO_x adsorption behaviour of Y-DOBDC-based MOF (yttrium-2,5-dihydroxyter-ephthalic acid) by analysing its photoluminescence (PL) characteristics in both pre- NO_x and post- NO_x exposures. As demonstrated in **Figure 1c**, the colour of synthesised Y-DOBDC-based MOF changed from pale yellow to vibrant brown–orange after NO_x exposure for 24 h under visible light. In addition, a significant reduction in the emission intensity of all compounds was observed under UV light illumination (350 nm) after 24 h exposure (**Figure 1d**), indicating the interaction between the DOBDC ligand in Y-DOBDC and NO_2 molecules (**Figure 1d**, inset). Observed and detectable optical signals upon the absorption of NO_2 gas provided a unique and direct means for NO_2 detection; however, quantitative analysis of the variable of NO_2 concentration was not addressed in detail [79].

3. Hydrogen Sulphide (H_2S)

H_2S is another air pollutant gas formed in large quantities by a range of activities, including some common large-scale activities such as sewerage processing and oil refining. In humans, H_2S can cause significant health concerns including allergic reactions and lung inflammation [80]. Despite significant advances in the design of highly sensitive H_2S gas sensors, continuous monitoring of trace-level (sub-ppm) H_2S at low operating temperatures is still challenging [81]. Given that H_2S is such a significant contaminant and is generated in several industrial applications, developing real-time sensitive and selective gas-sensing technologies for rapid detection of this gas is critical.

Zhang et al. [82] reported, for the first time, the fluorescence sensing of H_2S gas molecules through the post functionalisation of MIL-100(In) films with metal ions including Eu^{3+} and Cu^{2+} (**Figure 2a,b**). The sensing mechanism in this device was based on the reaction between Cu^{2+} ions and H_2S gas molecules, resulting in the activation of Eu^{3+} emission (**Figure 2c**). The fluorescence response of the MIL-100(In)@ $\text{Eu}^{3+}/\text{Cu}^{2+}$ film with a range of H_2S concentrations at an operating temperature of 40 °C is presented in **Figure 2d,e**. The fluorescence intensity of MIL-100(In)@ $\text{Eu}^{3+}/\text{Cu}^{2+}$ was found to increase steadily with the increase in H_2S level from 0 to 115 ppm (**Figure 2d**), with a linear increase in the luminescence intensity as a function of H_2S level (**Figure 2e**), and a detection limit of 0.535 ppm.

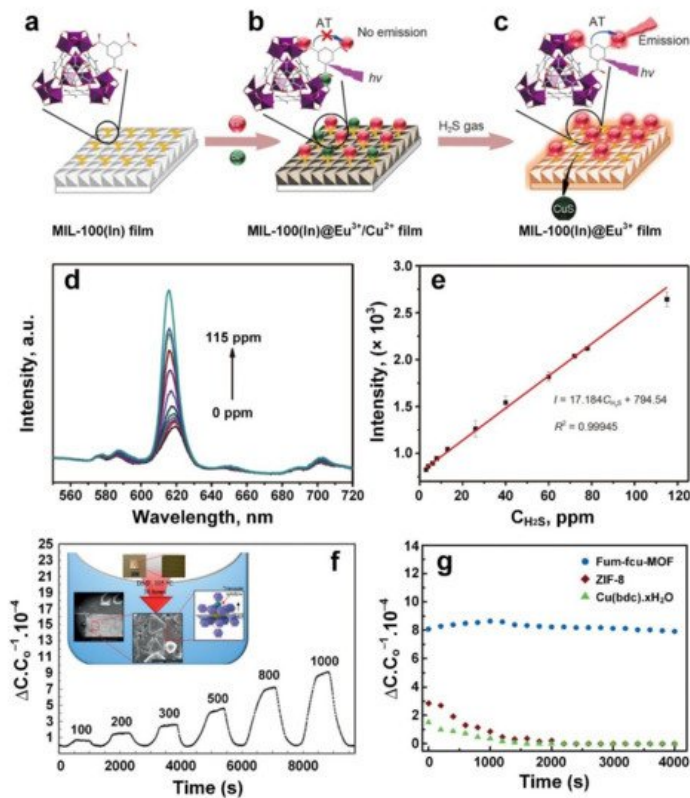


Figure 2. Schematic illustrations of MIL-100(In) based fluorescence sensor for H₂S gas detection: The MIL-100(In) film coordinating BTC ligands on the surface (a) can be functionalized by Eu³⁺/Cu²⁺ ions simultaneously with no emission of Eu³⁺ (b); however, the characteristic emission of Eu³⁺ in MIL-100(In)@Eu³⁺/Cu²⁺ film could turn on with the presence of H₂S gas (c). (d,e) Fluorescence intensity versus H₂S gas at different concentrations at 40 °C. Reproduced with permission from [82] Springer, 2019. (f) The dynamic response curves of fum-fcu-MOF against H₂S gas at different concentrations, and the microstructure of fum-fcu-MOF coated on IDE (Inset). (g) The stability performance of fum-fcu-MOF against ZIF-8 and Cu(BDC)·xH₂O MOF. Reproduced with permission from [83] Wiley-VCH, 2016.

4. Sulphur Dioxide (SO₂)

Very recently, Zhang et al. [28] developed a capacitive-based sensing material using a relatively simple fabrication process (Figure 3a) for the real-time monitoring of SO₂ gas molecules at room temperature. The sensing technology was introduced by using polyvinylidene fluoride (PVDF) nanofibers (with a diameter of 300–400 nm) coated with a thin layer of UiO-66-NH₂ MOF (200 nm in size) (Figure 3b, inset) as a dielectric layer and carbon nanotubes (CNTs) as an electrode. The fabricated sensing material demonstrated a high sensitivity towards SO₂ in a large ppm range from 1 ppm to 150 ppm (Figure 3b), high stability (over a testing period of 20 days) (Figure 3c) and excellent bending flexibility (2000 bending cycles), with a short response time of 185 s for detecting a low concentration of SO₂ gas. The sensing mechanism was based on the change in the dielectric constant of UiO-66-NH₂ MOF layer due to the physical adsorption of SO₂ gas molecules in the MOF pores and voids. Interestingly, it demonstrated a faster response dynamic (both response and recovery time) after bending (compared to an unbended sample), which could be attributed to the shortened distance between the electrode and dielectric layer, resulting in a shorter transfer path for gas molecules to reach the dielectric layer, and consequently faster response dynamics.

Using a simple solvothermal technique, Chernikova et al. [84] deposited a layer of MFM-300 (a 3-periodic open framework composing of InO₄(OH)₂ octahedral chains bridged by tetradentate ligands (biphenyl-3,3',5,5'-tetracarboxylic acid)) (Figure 3d), on a silicon wafer featuring a capacitive interdigitated electrode functionalized with 11-Mercapto-1-undecanol, for the low concentration detection of SO₂ gas molecules. The sensing performance of the proposed porous nanostructured layer (Figure 3e, inset) was investigated by monitoring the changes in capacitance upon exposure to a selection of different gas molecules including SO₂, CH₄, CO₂, NO₂ and H₂. The results showed outstanding detection sensitivity to SO₂ down to 75 ppb with a lower detection limit of 5 ppb and excellent selectivity towards SO₂ compared to other gases with slight cross-selectivity with CO₂ (four times less sensitive compared to SO₂).

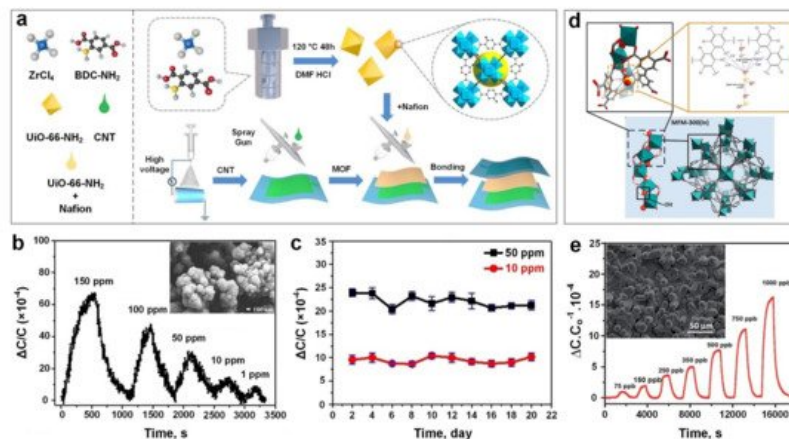


Figure 3. (a) Schematic illustrations of UiO-66-NH₂ preparation on flexible PVDF layer for capacitive SO₂ gas sensor. (b) The dynamic capacitance variations of UiO-66-NH₂ versus different SO₂ gas concentrations, and the SEM image of UiO-66-NH₂ powder (Inset). (c) The stability tests of UiO-66-NH₂ based gas sensor under 10 and 50 ppm of SO₂ gas for over 20 days. Reproduced with permission from [28] Wiley-VCH, 2021. (d) The structure of MFM-300 (In) MOF and the sites for SO₂ adsorption. (e) The capacitive response of MFM-300 (In) MOF against varied SO₂ gas concentrations, and the SEM image of MFM-300 (In) MOF thin film as inset. Reproduced with permission from [84] The Royal Society of Chemistry, 2018.

The effect of humidity level on sensing performance of the active film upon SO₂ exposure was investigated at 1000 and 350 ppb gas concentrations, and at relative humidity (RH) from 5% to 85%. In contrast to conventional gas sensors including metal oxide semiconductors, the sensing performance of the MFM-300-based gas sensor was enhanced significantly by increasing the RH up to 85%. This higher sensing response was attributed to the formation of additional hydrogen bonding between SO₂ gas molecules and adsorbed water molecules on the MOF's surface, resulting in a higher capacitance change [85][86]. In addition, the MFM-300 layer demonstrated a higher sensing performance at lower operating temperature with an optimal operating temperature of 22 °C, making it a promising material for highly sensitive, room temperature nanosensors for the ultra-low concentration detection of SO₂ gas molecules. This higher sensitivity could be attributed to a lower molecule diffusion rate and consequently, a higher analyte adsorption rate at a lower temperature [84].

In another approach, Ingle et al. [87] fabricated a flexible SO₂ gas sensor based on a crystalline nickel (II) benzenetricarboxylate metal-organic framework (Ni-MOF). In this device, the Ni-MOF composited with hydroxyl group (-OH) activated single-wall carbon nanotubes (SWNTs) and multi-wall carbon nanotubes (MWNTs), namely, Ni-MOF/-OH-SWNTs and Ni-MOF/-OH-MWNTs. Both CNT-modified Ni-MOF microdevices exhibited a discriminating response upon SO₂ exposure, which was contributed by the highly sensitive surface network of CNTs [88] providing favourable conditions for electron transportation [89]. The Ni-MOF/-OH-SWNTs sensor showed higher SO₂ sensing performance compared to the Ni-MOF/-OH-MWNTs at different SO₂ concentrations. This was due to holes being the majority charge carriers in Ni-MOF/-OH-SWNTs [90] resulting in better interaction with electron donor analytes such as SO₂ gas molecules. However, a slow recovery speed was observed which could be attributed to the honeycomb structure of the CNTs as this plays a significant role in holding the gas molecules on the sensor's surface for a longer time [89][91] prolonging the recovery dynamics of the device. A high sensing selectivity towards SO₂ molecules was also achieved using the MOF/CNT composite material compared to other gases, including NO₂, NH₃ and CO gases, at relatively high concentrations (≥10 ppm).

5. Carbon Dioxide (CO₂)

Despite the modest greenhouse effect of CO₂ compared to methane (CH₄) and nitrous oxide (N₂O), which possess 25 and 298 times more global warming potential (GWP) than CO₂, respectively [92][93], CO₂ is widely understood to be the major driver of climate change due to its dominant concentrations in the atmosphere (0.04 vol%) when compared to other types of greenhouse gas [94]. Sustained exposure to CO₂ gas indoors can cause inflammation and oxidative stress at a modest concentration level of 1000 ppm [95][96]. Thus, ongoing monitoring of indoor and outdoor CO₂ gas levels with reliable, portable and cost-effective sensing systems is highly desired in many industrial sectors.

The sensing performance of the MOF film was investigated by measuring the capacitance change upon exposure to different gases including methane, benzene and CO₂, resulting in an outstanding sensing response of ~1 towards 200 ppm CO₂ vapour (Figure 4e). This response is attributed to the interaction between unsaturated open metal sites of the

Mg-MOF-74 crystallites (as an electron acceptor) and adsorbed CO₂ molecules acting as electron donors. A positive linear response was reported upon increasing the CO₂ gas concentration from 200 to 5000 ppm and attributed to the linear change in the dielectric constant of the Mg-MOF-74 layer over the gas adsorption on the surface (**Figure 4e**, inset). However, no obvious response was detected for other gases, including methane, at similar concentrations. Post-synthesis modification of these MOF layers with ethylenediamine slightly increased their sensitivity towards CO₂. However, further investigations are required to reveal the key factors in the sensing performance of Mg-MOF-74 crystallites and their surface-analyte interaction with different gas molecules.

(a) Photograph of Mg-MOF-74 film-based CO₂ capacitive gas sensor. (b) Optical image of Pt IDEs. (c ,d) SEM images of the top (c) and side (d) views of the as-grown Mg-MOF-74 film on IDEs. (e) The dynamic response of ethylenediamine-modified Mg-MOF-74 film against CO₂ at different concentrations, the response varied proportionally to the CO₂ concentration (inset). Reproduced with permission from [91] Wiley-VCH, 2019. (f) CO₂ adsorption isotherms of Co-MOF-74 (i) and Co-MOF-74-TTF (ii). (g) The I-V curves of Co-MOF-74-TTF under CO₂ and other atmospheric conditions. Reproduced with permission from [92] American Chemical Society, 2019. (h) The normalized dynamic response curves and, (i) response versus CO₂ gas at different concentrations for various humidity scenarios (0–80% RH). Reproduced with permission from [93] American Chemical Society, 2019.

To investigate the gas-sensing capability of Co-MOF-74-TTF, the I-V characteristics of the sensing material was measured after 24 h under vacuum, air, N₂, CH₄, and CO₂ atmospheres, respectively, at an applied voltage up to 10 V. The material demonstrated a higher sensing performance towards CO₂ gas molecules (current of 7 nA) compared to other gases including CH₄ (current of 6 nA) and N₂ (current of 4.5 nA) at 10 V (**Figure 4g**). This higher sensing performance could be attributed to the strong interaction between open-metal Co-centres (acting as the Lewis acid) of MOF and CO₂ gas molecules (acting as the Lewis base/electron donor) resulting in the highest conductivity of the fabricated sensing material upon exposure to CO₂ gas (**Figure 4g**), while a smaller increase in the conductivity was observed for weaker gas-MOF interactions (CO₂ > CH₄ > N₂). In fact, the permanent dipole moment, which is present in the cobalt atoms, could induce the polarization of molecules such as CH₄, resulting in the lower affinity of Co-MOF-74 toward CH₄ compared to CO₂ [93]. In addition, a significantly lower interaction was expected for N₂, as an inert gas, resulting in a lower sensing response towards N₂ gas molecules. Further investigation is required to resolve the poor selectivity and slow response dynamics (>500 min) of these Co-MOF-74-TTF for their real-world application as CO₂ gas sensors [92].

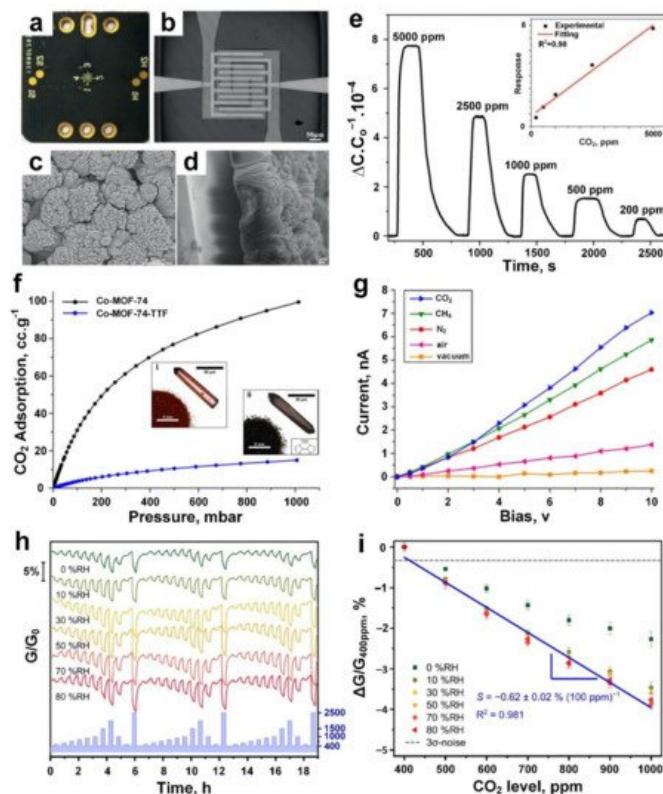


Figure 4. (a) Photograph of Mg-MOF-74 film-based CO₂ capacitive gas sensor. (b) Optical image of Pt IDEs. (c,d) SEM images of the top (c) and side (d) views of the as-grown Mg-MOF-74 film on IDEs. (e) The dynamic response of ethylenediamine-modified Mg-MOF-74 film against CO₂ at different concentrations, the response varied proportionally to the CO₂ concentration (inset). Reproduced with permission from [91] Wiley-VCH, 2019. (f) CO₂ adsorption isotherms of Co-MOF-74 (i) and Co-MOF-74-TTF (ii). (g) The I-V curves of Co-MOF-74-TTF under CO₂ and other atmospheric conditions. Reproduced with permission from [92] American Chemical Society, 2019. (h) The normalized dynamic response curves and (i) response versus CO₂ gas at different concentrations for various humidity scenarios (0–80% RH). Reproduced with permission from [93] American Chemical Society, 2019.

and, (i) response versus CO₂ gas at different concentrations for various humidity scenarios (0–80% RH). Reproduced with permission from [98] American Chemical Society, 2019.

6. Summary and Outlook

High sensitivity and selectivity at low operating temperatures have been reported for state-of-the-art MOF-based sensors making them a promising candidate for various gas-sensing applications; however, MOF-based nanosensors for sub-ppb detection of gas molecules are still in the initial stages of development, with much room to improve the sensing performance of these MOF materials and many opportunities to enhance their LODs towards gas molecules.

High chemical, thermal, and photo stabilities have been achieved for some of the MOF-based sensing technologies, which determine their repeatability and long-term reusability. However, recent studies have indicated that some of the widely used MOFs for gas sensors undergo partial degradation upon exposure to moisture. Continued efforts are necessary for the design and development of robust MOF-based sensing materials to demonstrate long-term stability in different environments. Careful assessment of MOF sensors after long-term tests using analytical techniques sensitive to MOF degradation will enable researchers to improve their stability. The careful design of novel MOF structures (such as mixed metal ions, hydrophobic ligands, and interpenetration of frameworks), post-processing of current MOFs (such as metal/ligand exchange, hydrophobic surface modification, and thermal treatment), and compositing MOFs with, or encapsulating MOFs into, other materials (such as polymers, carbon nanotubes, graphenes and graphene oxide) are among the proposed techniques for improving the chemical stability of MOFs.

The inherently low electrical conductivity of most MOFs has severely limited their applications in gas and liquid sensors. However, the development of highly porous 2D conductive MOFs with tunable cavity size has facilitated the rise of MOF-based sensing technologies. In addition, the design of novel nanomaterials, including guest-MOF nanostructures where MOFs and guest molecules are combined, has shown excellent enhancement in the conductivity of MOF-based gas sensors.

The future is bright for the development of highly sensitive and selective MOF-based nanosensors for room temperature detection of low concentrations of gas molecules, with applications in many areas of technology, industry, or daily life, providing strong health, safety and security benefits to address many standing fundamental and technological challenges.

References

1. Lustig, W.P.; Mukherjee, S.; Rudd, N.D.; Desai, A.V.; Li, J.; Ghosh, S.K. Metal–organic frameworks: Functional luminescent and photonic materials for sensing applications. *Chem. Soc. Rev.* 2017, 46, 3242–3285.
2. Fang, X.; Zong, B.; Mao, S. Metal–Organic Framework-Based Sensors for Environmental Contaminant Sensing. *Nano-Micro Lett.* 2018, 10, 64.
3. Zhou, X.; Xue, Z.; Chen, X.; Huang, C.; Bai, W.; Lu, Z.; Wang, T. Nanomaterial-based gas sensors used for breath diagnosis. *J. Mater. Chem. B* 2020, 8, 3231–3248.
4. Nasiri, N.; Clarke, C. Nanostructured Gas Sensors for Medical and Health Applications: Low to High Dimensional Materials. *Biosensors* 2019, 9, 43.
5. Nasiri, N.; Clarke, C. Nanostructured Chemiresistive Gas Sensors for Medical Applications. *Sensors* 2019, 19, 462.
6. Chen, X.; Leishman, M.; Bagnall, D.; Nasiri, N. Nanostructured Gas Sensors: From Air Quality and Environmental Monitoring to Healthcare and Medical Applications. *Nanomaterials* 2021, 11, 1927.
7. Korotcenkov, G.; Cho, B.K. Metal oxide composites in conductometric gas sensors: Achievements and challenges. *Sens. Actuators B Chem.* 2017, 244, 182–210.
8. Li, H.-Y.; Zhao, S.-N.; Zang, S.-Q.; Li, J. Functional metal-organic frameworks as effective sensors of gases and volatile compounds. *Chem. Soc. Rev.* 2020, 49, 6364–6401.
9. Yuan, H.; Tao, J.; Li, N.; Karmakar, A.; Tang, C.; Cai, H.; Pennycook, S.J.; Singh, N.; Zhao, D. On-Chip Tailorability of Capacitive Gas Sensors Integrated with Metal–Organic Framework Films. *Angew. Chem.* 2019, 131, 14227–14232.
10. Wang, H.; Lustig, W.P.; Li, J. Sensing and capture of toxic and hazardous gases and vapors by metal–organic frameworks. *Chem. Soc. Rev.* 2018, 47, 4729–4756.
11. Rasheed, T.; Nabeel, F. Luminescent metal-organic frameworks as potential sensory materials for various environmental toxic agents. *Coord. Chem. Rev.* 2019, 401, 213065.

12. Wenger, O.S. Vapochromism in Organometallic and Coordination Complexes: Chemical Sensors for Volatile Organic Compounds. *Chem. Rev.* 2013, 113, 3686–3733.
13. Dolgoplova, E.A.; Rice, A.M.; Martin, C.R.; Shustova, N.B. Photochemistry and photophysics of MOFs: Steps towards MOF-based sensing enhancements. *Chem. Soc. Rev.* 2018, 47, 4710–4728.
14. Yan, B. Lanthanide-Functionalized Metal–Organic Framework Hybrid Systems to Create Multiple Luminescent Centers for Chemical Sensing. *Acc. Chem. Res.* 2017, 50, 2789–2798.
15. Wang, X.-D.; Wolfbeis, O.S. Optical methods for sensing and imaging oxygen: Materials, spectroscopies and applications. *Chem. Soc. Rev.* 2014, 43, 3666–3761.
16. Dey, A. Semiconductor metal oxide gas sensors: A review. *Mater. Sci. Eng. B Solid-State Mater. Adv. Technol.* 2018, 229, 206–217.
17. Hu, Z.; Deibert, B.J.; Li, J. Luminescent metal–organic frameworks for chemical sensing and explosive detection. *Chem. Soc. Rev.* 2014, 43, 5815–5840.
18. Karmakar, A.; Samanta, P.; Desai, A.V.; Ghosh, S.K. Guest-Responsive Metal–Organic Frameworks as Scaffolds for Separation and Sensing Applications. *Acc. Chem. Res.* 2017, 50, 2457–2469.
19. Stassen, I.; Burtch, N.; Talin, A.; Falcaro, P.; Allendorf, M.; Ameloot, R. An updated roadmap for the integration of metal–organic frameworks with electronic devices and chemical sensors. *Chem. Soc. Rev.* 2017, 46, 3185–3241.
20. Wales, D.J.; Grand, J.; Ting, V.P.; Burke, R.D.; Edler, K.J.; Bowen, C.R.; Mintova, S.; Burrows, A.D. Gas sensing using porous materials for automotive applications. *Chem. Soc. Rev.* 2015, 44, 4290–4321.
21. Kreno, L.E.; Leong, K.; Farha, O.K.; Allendorf, M.; Van Duyne, R.P.; Hupp, J.T. Metal–Organic Framework Materials as Chemical Sensors. *Chem. Rev.* 2012, 112, 1105–1125.
22. Reglero Ruiz, J.; Sanjuán, A.; Vallejos, S.; García, F.; García, J. Smart Polymers in Micro and Nano Sensory Devices. *Chemosensors* 2018, 6, 12.
23. Ciprian, R.; Baratto, C.; Giglia, A.; Koshmak, K.; Vinai, G.; Donarelli, M.; Ferroni, M.; Campanini, M.; Comini, E.; Ponzoni, A.; et al. Magnetic gas sensing exploiting the magneto-optical Kerr effect on ZnO nanorods/Co layer system. *RSC Adv.* 2016, 6, 42517–42521.
24. Matatagui, D.; Kolokoltsev, O.V.; Qureshi, N.; Mejía-Urriarte, E.V.; Saniger, J.M. A magnonic gas sensor based on magnetic nanoparticles. *Nanoscale* 2015, 7, 9607–9613.
25. Zou, C.W.; Wang, J.; Liang, F.; Xie, W.; Shao, L.X.; Fu, D.J. Large-area aligned CuO nanowires arrays: Synthesis, anomalous ferromagnetic and CO gas sensing properties. *Curr. Appl. Phys.* 2012, 12, 1349–1354.
26. Impeng, S.; Junkaew, A.; Maitarad, P.; Kungwan, N.; Zhang, D.; Shi, L.; Namuangruk, S. A Mn₄ moiety embedded graphene as a magnetic gas sensor for CO detection: A first principle study. *Appl. Surf. Sci.* 2019, 473, 820–827.
27. Zhu, C.; Gerald, R.E.; Huang, J. Metal-organic Framework Materials Coupled to Optical Fibers for Chemical Sensing: A Review. *IEEE Sens. J.* 2021, 1.
28. Zhang, X.; Zhai, Z.; Wang, J.; Hao, X.; Sun, Y.; Yu, S.; Lin, X.; Qin, Y.; Li, C. Zr-MOF Combined with Nanofibers as an Efficient and Flexible Capacitive Sensor for Detecting SO₂. *ChemNanoMat* 2021.
29. Zhai, Z.; Zhang, X.; Hao, X.; Niu, B.; Li, C. Metal–Organic Frameworks Materials for Capacitive Gas Sensors. *Adv. Mater. Technol.* 2021, 2100127.
30. Fernandez, E.; Saiz, P.G.; Peřinka, N.; Wuttke, S.; Fernández De Luis, R. Printed Capacitive Sensors Based on Ionic Liquid/Metal–Organic Framework Composites for Volatile Organic Compounds Detection. *Adv. Funct. Mater.* 2021, 31, 2010703.
31. Srinivas, C.; Ranjith Kumar, E.; Tirupanyam, B.V.; Singh Meena, S.; Bhatt, P.; Prajapat, C.L.; Chandrasekhar Rao, T.V.; Sastry, D.L. Study of magnetic behavior in co-precipitated Ni–Zn ferrite nanoparticles and their potential use for gas sensor applications. *J. Magn. Magn. Mater.* 2020, 502, 166534.
32. Sava Gallis, D.F.; Vogel, D.J.; Vincent, G.A.; Rimsza, J.M.; Nenoff, T.M. NO_x Adsorption and Optical Detection in Rare Earth Metal–Organic Frameworks. *ACS Appl. Mater. Interfaces* 2019, 11, 43270–43277.
33. Chen, H.; Bo, R.; Shrestha, A.; Xin, B.; Nasiri, N.; Zhou, J.; Di Bernardo, I.; Dodd, A.; Saunders, M.; Lipton-Duffin, J.; et al. NiO–ZnO Nanoheterojunction Networks for Room-Temperature Volatile Organic Compounds Sensing. *Adv. Opt. Mater.* 2018, 6, 1800677.
34. Gerber, A.; Kopnov, G.; Karpovski, M. Hall effect spintronics for gas detection. *Appl. Phys. Lett.* 2017, 111, 143505.
35. Alam, M.F.B.; Phan, D.-T.; Chung, G.-S. Palladium nanocubes decorated on a one-dimensional ZnO nanorods array for use as a hydrogen gas sensor. *Mater. Lett.* 2015, 156, 113–117.

36. Yang, S.; Lei, G.; Xu, H.; Lan, Z.; Wang, Z.; Gu, H. Metal Oxide Based Heterojunctions for Gas Sensors: A Review. *Nanomaterials* 2021, 11, 1026.
37. Zhang, J.; Qin, Z.; Zeng, D.; Xie, C. Metal-oxide-semiconductor based gas sensors: Screening, preparation, and integration. *Phys. Chem. Chem. Phys.* 2017, 19, 6313–6329.
38. Cichosz, S.; Masek, A.; Zaborski, M. Polymer-based sensors: A review. *Polym. Test.* 2018, 67, 342–348.
39. Fratoddi, I.; Venditti, I.; Cametti, C.; Russo, M.V. Chemiresistive polyaniline-based gas sensors: A mini review. *Sens. Actuators B Chem.* 2015, 220, 534–548.
40. Ding, B.; Yamazaki, M.; Shiratori, S. Electrospun fibrous polyacrylic acid membrane-based gas sensors. *Sens. Actuators B Chem.* 2005, 106, 477–483.
41. Barauskas, D.; Pelenis, D.; Vanagas, G.; Viržonis, D.; Baltrušaitis, J. Methylated Poly(ethyleneimine) Modified Capacitive Micromachined Ultrasonic Transducer for Measurements of CO₂ and SO₂ in Their Mixtures. *Sensors* 2019, 19, 3236.
42. Gargiulo, V.; Alfano, B.; Di Capua, R.; Alfé, M.; Vorokhta, M.; Polichetti, T.; Massera, E.; Miglietta, M.L.; Schiattarella, C.; Di Francia, G. Graphene-like layers as promising chemiresistive sensing material for detection of alcohols at low concentration. *J. Appl. Phys.* 2018, 123, 024503.
43. Li, C.; Wang, Y.; Jiang, H.; Wang, X. Review—Intracellular Sensors Based on Carbonaceous Nanomaterials: A Review. *J. Electrochem. Soc.* 2020, 167, 037540.
44. Wang, Y.; Yeow, J.T.W. A Review of Carbon Nanotubes-Based Gas Sensors. *J. Sens.* 2009, 2009, 493904.
45. Zhang, T.; Mubeen, S.; Myung, N.V.; Deshusses, M.A. Recent progress in carbon nanotube-based gas sensors. *Nanotechnology* 2008, 19, 332001.
46. Llobet, E. Gas sensors using carbon nanomaterials: A review. *Sens. Actuators B Chem.* 2013, 179, 32–45.
47. Lee, J.M.; Park, J.-E.; Kim, S.; Kim, S.; Lee, E.; Kim, S.-J.; Lee, W. Ultra-sensitive hydrogen gas sensors based on Pd-decorated tin dioxide nanostructures: Room temperature operating sensors. *Int. J. Hydrog. Energy* 2010, 35, 12568–12573.
48. Sharma, B.; Kim, J.-S. Graphene decorated Pd-Ag nanoparticles for H₂ sensing. *Int. J. Hydrog. Energy* 2018, 43, 11397–11402.
49. Zhang, S.; Yang, M.; Liang, K.; Turak, A.; Zhang, B.; Meng, D.; Wang, C.; Qu, F.; Cheng, W.; Yang, M. An acetone gas sensor based on nanosized Pt-loaded Fe₂O₃ nanocubes. *Sens. Actuators B Chem.* 2019, 290, 59–67.
50. Barbosa, M.S.; Suman, P.H.; Kim, J.J.; Tuller, H.L.; Orlandi, M.O. Investigation of electronic and chemical sensitization effects promoted by Pt and Pd nanoparticles on single-crystalline SnO nanobelt-based gas sensors. *Sens. Actuators B Chem.* 2019, 301, 127055.
51. Gębicki, J.; Kloskowski, A.; Chrzanowski, W.; Stepnowski, P.; Namiesnik, J. Application of Ionic Liquids in Amperometric Gas Sensors. *Crit. Rev. Anal. Chem.* 2016, 46, 122–138.
52. Paul, A.; Muthukumar, S.; Prasad, S. Room-temperature ionic liquids for electrochemical application with special focus on gas sensors. *J. Electrochem. Soc.* 2019, 167, 037511.
53. Zevenbergen, M.A.G.; Wouters, D.; Dam, V.-A.T.; Brongersma, S.H.; Crego-Calama, M. Electrochemical Sensing of Ethylene Employing a Thin Ionic-Liquid Layer. *Anal. Chem.* 2011, 83, 6300–6307.
54. Li, Y.; Xiao, A.-S.; Zou, B.; Zhang, H.-X.; Yan, K.-L.; Lin, Y. Advances of metal–organic frameworks for gas sensing. *Polyhedron* 2018, 154, 83–97.
55. Kumar, P.; Deep, A.; Kim, K.-H. Metal organic frameworks for sensing applications. *TrAC—Trends Anal. Chem.* 2015, 73, 39–53.
56. Hu, M.-L.; Razavi, S.A.A.; Piroozzadeh, M.; Morsali, A. Sensing organic analytes by metal–organic frameworks: A new way of considering the topic. *Inorg. Chem. Front.* 2020, 7, 1598–1632.
57. Abideen, Z.U.; Kim, J.-H.; Lee, J.-H.; Kim, J.-Y.; Mirzaei, A.; Kim, H.W.; Kim, S.S. Electrospun Metal Oxide Composite Nanofibers Gas Sensors: A Review. *J. Korean Ceram. Soc.* 2017, 54, 366–379.
58. Wang, C.; Wang, Y.; Yang, Z.; Hu, N. Review of recent progress on graphene-based composite gas sensors. *Ceram. Int.* 2021, 47, 16367–16384.
59. Love, C.; Nazemi, H.; El-Masri, E.; Ambrose, K.; Freund, M.S.; Emadi, A. A Review on Advanced Sensing Materials for Agricultural Gas Sensors. *Sensors* 2021, 21, 3423.
60. Mirzaei, A.; Leonardi, S.G.; Neri, G. Detection of hazardous volatile organic compounds (VOCs) by metal oxide nanostructures-based gas sensors: A review. *Ceram. Int.* 2016, 42, 15119–15141.

61. Wang, J.; Shen, H.; Xia, Y.; Komarneni, S. Light-activated room-temperature gas sensors based on metal oxide nanostructures: A review on recent advances. *Ceram. Int.* 2021, 47, 7353–7368.
62. Amiri, V.; Roshan, H.; Mirzaei, A.; Neri, G.; Ayesh, A.I. Nanostructured Metal Oxide-Based Acetone Gas Sensors: A Review. *Sensors* 2020, 20, 3096.
63. Wang, C.; Yin, L.; Zhang, L.; Xiang, D.; Gao, R. Metal Oxide Gas Sensors: Sensitivity and Influencing Factors. *Sensors* 2010, 10, 2088–2106.
64. Moseley, P.T. Progress in the development of semiconducting metal oxide gas sensors: A review. *Meas. Sci. Technol.* 2017, 28, 082001.
65. Adhikari, B.; Majumdar, S. Polymers in sensor applications. *Prog. Polym. Sci.* 2004, 29, 699–766.
66. Song, L.-F.; Jiang, C.-H.; Jiao, C.-L.; Zhang, J.; Sun, L.-X.; Xu, F.; You, W.-S.; Wang, Z.-G.; Zhao, J.-J. Two New Metal–Organic Frameworks with Mixed Ligands of Carboxylate and Bipyridine: Synthesis, Crystal Structure, and Sensing for Methanol. *Cryst. Growth Des.* 2010, 10, 5020–5023.
67. Achmann, S.; Hagen, G.; Kita, J.; Malkowsky, I.; Kiener, C.; Moos, R. Metal-Organic Frameworks for Sensing Applications in the Gas Phase. *Sensors* 2009, 9, 1574–1589.
68. Yao, M.-S.; Lv, X.-J.; Fu, Z.-H.; Li, W.-H.; Deng, W.-H.; Wu, G.-D.; Xu, G. Layer-by-Layer Assembled Conductive Metal-Organic Framework Nanofilms for Room-Temperature Chemiresistive Sensing. *Angew. Chem.* 2017, 129, 16737–16741.
69. Arul, C.; Moulae, K.; Donato, N.; Iannazzo, D.; Lavanya, N.; Neri, G.; Sekar, C. Temperature modulated Cu-MOF based gas sensor with dual selectivity to acetone and NO₂ at low operating temperatures. *Sens. Actuators B Chem.* 2021, 329.
70. Koo, W.T.; Jang, J.S.; Kim, I.D. Metal-Organic Frameworks for Chemiresistive Sensors. *Chem* 2019, 5, 1938–1963.
71. Lai, C.; Wang, Z.; Qin, L.; Fu, Y.; Li, B.; Zhang, M.; Liu, S.; Li, L.; Yi, H.; Liu, X.; et al. Metal-organic frameworks as burgeoning materials for the capture and sensing of indoor VOCs and radon gases. *Coord. Chem. Rev.* 2021, 427, 213565.
72. Gaba, A.; Felicia, S. Reduction of Air Pollution by Combustion Processes. In *The Impact of Air Pollution on Health, Economy, Environment and Agricultural Sources*; InTech: London, UK, 2011; pp. 119–142.
73. WHO. Air Quality Guidelines for Particulate Matter, Ozone, Nitrogen Dioxide and Sulfur Dioxide: Global Update 2005; WHO: Geneva, Switzerland, 2006.
74. Chen, T.-M.; Kuschner, W.G.; Gokhale, J.; Shofer, S. Outdoor Air Pollution: Nitrogen Dioxide, Sulfur Dioxide, and Carbon Monoxide Health Effects. *Am. J. Med. Sci.* 2007, 333, 249–256.
75. Gamonal, A.; Sun, C.; Mariano, A.L.; Fernandez-Bartolome, E.; Guerrero-Sanvicente, E.; Vlaisavljevich, B.; Castells-Gil, J.; Marti-Gastaldo, C.; Poloni, R.; Wannemacher, R.; et al. Divergent Adsorption-Dependent Luminescence of Amino-Functionalized Lanthanide Metal–Organic Frameworks for Highly Sensitive NO₂ Sensors. *J. Phys. Chem. Lett.* 2020, 11, 3362–3368.
76. Zhang, J.; Hu, E.; Liu, F.; Li, H.; Xia, T. Growth of robust metal–organic framework films by spontaneous oxidation of a metal substrate for NO₂ sensing. *Mater. Chem. Front.* 2021.
77. Moscoso, F.G.; Almeida, J.; Sousaraei, A.; Lopes-Costa, T.; Silva, A.M.G.; Cabanillas-Gonzalez, J.; Cunha-Silva, L.; Pedrosa, J.M. Luminescent MOF crystals embedded in PMMA/PDMS transparent films as effective NO₂ gas sensors. *Mol. Syst. Des. Eng.* 2020, 5, 1048–1056.
78. Kim, J.-O.; Koo, W.-T.; Kim, H.; Park, C.; Lee, T.; Hutomo, C.A.; Choi, S.Q.; Kim, D.S.; Kim, I.-D.; Park, S. Large-area synthesis of nanoscopic catalyst-decorated conductive MOF film using microfluidic-based solution shearing. *Nat. Commun.* 2021, 12.
79. Ma, Y.-X.; Gao, B.; Li, Y.; Wei, W.; Zhao, Y.; Ma, J.-F. Macrocyclic-Based Metal–Organic Frameworks with NO₂-Driven On/Off Switch of Conductivity. *ACS Appl. Mater. Interfaces* 2021, 13, 27066–27073.
80. Meng, C.; Cui, X.; Qi, S.; Zhang, J.; Kang, J.; Zhou, H. Lung inflation with hydrogen sulfide during the warm ischemia phase ameliorates injury in rat donor lungs via metabolic inhibition after cardiac death. *Surgery* 2017, 161, 1287–1298.
81. Zhou, X.; Lin, X.; Yang, S.; Zhu, S.; Chen, X.; Dong, B.; Bai, X.; Wen, X.; Geyu, L.; Song, H. Highly dispersed Metal–Organic-Framework-Derived Pt nanoparticles on three-dimensional macroporous ZnO for trace-level H₂S sensing. *Sens. Actuators B Chem.* 2020, 309, 127802.
82. Zhang, J.; Liu, F.; Gan, J.; Cui, Y.; Li, B.; Yang, Y.; Qian, G. Metal-organic framework film for fluorescence turn-on H₂S gas sensing and anti-counterfeiting patterns. *Sci. China Mater.* 2019, 62, 1445–1453.

83. Yassine, O.; Shekhah, O.; Assen, A.H.; Belmabkhout, Y.; Salama, K.N.; Eddaoudi, M. H₂S Sensors: Fumarate-Based fcu-MOF Thin Film Grown on a Capacitive Interdigitated Electrode. *Angew. Chem.* 2016, 128, 16111–16115.
84. Chernikova, V.; Yassine, O.; Shekhah, O.; Eddaoudi, M.; Salama, K.N. Highly sensitive and selective SO₂ MOF sensor: The integration of MFM-300 MOF as a sensitive layer on a capacitive interdigitated electrode. *J. Mater. Chem. A* 2018, 6, 5550–5554.
85. Assen, A.H.; Yassine, O.; Shekhah, O.; Eddaoudi, M.; Salama, K.N. MOFs for the Sensitive Detection of Ammonia: Deployment of fcu-MOF Thin Films as Effective Chemical Capacitive Sensors. *ACS Sens.* 2017, 2, 1294–1301.
86. Sapsanis, C.; Omran, H.; Chernikova, V.; Shekhah, O.; Belmabkhout, Y.; Buttner, U.; Eddaoudi, M.; Salama, K. Insights on Capacitive Interdigitated Electrodes Coated with MOF Thin Films: Humidity and VOCs Sensing as a Case Study. *Sensors* 2015, 15, 18153–18166.
87. Ingle, N.; Sayyad, P.; Deshmukh, M.; Bodkhe, G.; Mahadik, M.; Al-Gahouari, T.; Shirsat, S.; Shirsat, M.D. A chemiresistive gas sensor for sensitive detection of SO₂ employing Ni-MOF modified –OH-SWNTs and –OH-MWNTs. *Appl. Phys. A* 2021, 127.
88. Seesaard, T.; Kerdcharoen, T.; Wongchoosuk, C. Hybrid materials with carbon nanotubes for gas sensing. In *Semiconductor Gas Sensors*, 2nd ed.; Jaaniso, R., Tan, O.K., Eds.; Woodhead Publishing: Sawston, UK, 2020; pp. 185–222.
89. Ma, P.-C.; Liu, M.-Y.; Zhang, H.; Wang, S.-Q.; Wang, R.; Wang, K.; Wong, Y.-K.; Tang, B.-Z.; Hong, S.-H.; Paik, K.-W.; et al. Enhanced Electrical Conductivity of Nanocomposites Containing Hybrid Fillers of Carbon Nanotubes and Carbon Black. *ACS Appl. Mater. Interfaces* 2009, 1, 1090–1096.
90. Ingle, N.; Mane, S.; Sayyad, P.; Bodkhe, G.; Al-Gahouari, T.; Mahadik, M.; Shirsat, S.; Shirsat, M.D. Sulfur Dioxide (SO₂) Detection Using Composite of Nickel Benzene Carboxylic (Ni3BTC₂) and OH-Functionalized Single Walled Carbon Nanotubes (OH-SWNTs). *Front. Mater. Sci.* 2020, 7, 93.
91. Mao, S.; Lu, G.; Chen, J. Nanocarbon-based gas sensors: Progress and challenges. *J. Mater. Chem. A* 2014, 2, 5573.
92. Boucher, O.; Friedlingstein, P.; Collins, B.; Shine, K.P. The indirect global warming potential and global temperature change potential due to methane oxidation. *Environ. Res. Lett.* 2009, 4, 044007.
93. Hou, H.; Peng, S.; Xu, J.; Yang, S.; Mao, Z. Seasonal variations of CH₄ and N₂O emissions in response to water management of paddy fields located in Southeast China. *Chemosphere* 2012, 89, 884–892.
94. Ritchie, H.; Roser, M. CO₂ and Greenhouse Gas Emission. Available online: <https://ourworldindata.org/co2-and-other-greenhouse-gas-emissions> (accessed on 22 August 2021).
95. Ramalho, O.; Wyart, G.; Mandin, C.; Blondeau, P.; Cabanes, P.-A.; Leclerc, N.; Mullot, J.-U.; Boulanger, G.; Redaelli, M. Association of carbon dioxide with indoor air pollutants and exceedance of health guideline values. *Build Environ.* 2015, 93, 115–124.
96. Jacobson, T.A.; Kler, J.S.; Hernke, M.T.; Braun, R.K.; Meyer, K.C.; Funk, W.E. Direct human health risks of increased atmospheric carbon dioxide. *Nat. Sustain.* 2019, 2, 691–701.
97. Strauss, I.; Mundstock, A.; Treger, M.; Lange, K.; Hwang, S.; Chmelik, C.; Rusch, P.; Bigall, N.C.; Pichler, T.; Shiozawa, H.; et al. Metal–Organic Framework Co-MOF-74-Based Host–Guest Composites for Resistive Gas Sensing. *ACS Appl. Mater. Interfaces* 2019, 11, 14175–14181.
98. Stassen, I.; Dou, J.-H.; Hendon, C.; Dincă, M. Chemiresistive Sensing of Ambient CO₂ by an Autogenously Hydrated Cu₃(hexaiminobenzene)₂ Framework. *ACS Cent. Sci.* 2019, 5, 1425–1431.
99. García, E.J.; Mowat, J.P.S.; Wright, P.A.; Pérez-Pellitero, J.; Jallut, C.; Pirngruber, G.D. Role of Structure and Chemistry in Controlling Separations of CO₂/CH₄ and CO₂/CH₄/CO Mixtures over Honeycomb MOFs with Coordinatively Unsaturated Metal Sites. *J. Phys. Chem. C* 2012, 116, 26636–26648.